Magnetic Fields throughout Stellar Evolution
Proceedings IAU Symposium No. 302, 2013
P. Petit, M. Jardine & H. Spruit, eds.

doi:10.1017/S1743921314002634

Hall Effect in Neutron Star Crusts

K. N. Gourgouliatos[1] and A. Cumming[1]

[1]Department of Physics, McGill University, 3600 rue University, Montréal,
Québec H3A 2T8, Canada
email: kostasg@physics.mcgill.ca

Abstract. The crust of Neutron Stars can be approximated by a highly conducting solid crystal lattice. The evolution of the magnetic field in the crust is mediated through Hall effect, namely the electric current is carried by the free electrons of the lattice and the magnetic field lines are advected by the electron fluid. Here, we present the results of a time-dependent evolution code which shows the effect Hall drift has in the large-scale evolution of the magnetic field. In particular we link analytical predictions with simulation results. We find that there are two basic evolutionary paths, depending on the initial conditions compared to Hall equilibrium. We also show the effect axial symmetry combined with density gradient have on suppressing turbulent cascade.

Keywords. MHD, stars: magnetic field, stars: neutron

1. Introduction

The magnetic field of neutron stars is anchored in their crust. The crust is an electric conductor, where only electrons have the freedom to move with respect to the static lattice. As most observable properties of neutron stars are directly connected to processes of the magnetosphere and the surface of the neutron star, the understanding of the magnetic field evolution is crucial. Goldreich & Reisenegger (1992) have shown that the evolution of the magnetic field in neutron stars is governed by three processes: Hall drift, ambipolar diffusion and Ohmic dissipation. The relative importance of these processes depends primarily on the intensity of the magnetic field and the electron density, with Hall effect dominating in the crust for magnetic fields $B > 10^{13}$G, while ambipolar diffusion being important in the core where the neutron fraction is larger. The strongly magnetized and with low characteristic ages magnetars have dipole inferred magnetic fields reaching 10^{15}G (Olausen & Kaspi 2013), while older pulsars have weaker fields, suggesting some decay of the field with age.

The evolution of crustal magnetic field due to the Hall effect has been studied analytically (Jones 1988; Vainshtein *et al.* 2000; Reisenegger *et al.* 2007) and numerically (Shalybkov & Urpin 1997; Hollerbach & Rüdiger 2002, 2004; Pons & Geppert 2007; Viganò *et al.* 2012; Kojima & Kisaka 2012). However, there are still some open questions. In particular, it is important to link the analytical work with the results of the simulations, explore a variety of initial conditions and their effect in the structure of the field and investigate the absence of turbulent cascade in crust simulations as opposed to cartesian 3-D box simulations (Biskamp *et al.* 1996; Cho & Lazarian 2009; Wareing & Hollerbach 2009).

Here we present the results of a code we have developed examining the evolution of axially symmetric magnetic fields in neutron star crusts under the influence of the Hall effect and Ohmic dissipation.

2. Hall Effect

An axially symmetric magnetic field can be expressed using two scalar functions Ψ and I, $\boldsymbol{B} = \nabla\Psi \times \nabla\phi + I\nabla\phi$, where ϕ is the azimuthal angle. Since only electrons have the freedom to move, the electric current is given by $\boldsymbol{j} = -n_{\rm e}{\rm e}\boldsymbol{v}$, where $n_{\rm e}$ is the electron number density, e is the electron charge and $\boldsymbol{v}$ is the electron velocity. From Ampère's law it is $\boldsymbol{j} = \frac{c}{4\pi}\nabla \times \boldsymbol{B}$, where c is the speed of light, while for a finite conductivity σ the electric field becomes $\boldsymbol{E} = -\frac{1}{c}\boldsymbol{v} \times \boldsymbol{B} + \frac{1}{\sigma}\boldsymbol{j}$. We substitute the electric field in the induction equation and we find

$$\frac{\partial \boldsymbol{B}}{\partial t} = -\frac{c}{4\pi {\rm e}}\nabla \times \left(\frac{\nabla \times \boldsymbol{B}}{n_e} \times \boldsymbol{B}\right) - \frac{c^2}{4\pi}\nabla \times \left(\frac{\nabla \times \boldsymbol{B}}{\sigma}\right). \tag{2.1}$$

In spherical polar coordinates (r, θ, ϕ) we define the Grad-Shafranov operator $\Delta^* = \frac{\partial^2}{\partial r^2} + \frac{\sin\theta}{r^2}\frac{\partial}{\partial\theta}\left(\frac{1}{\sin\theta}\frac{\partial}{\partial\theta}\right)$ and $\chi = c/(4\pi {\rm e} n_{\rm e} r^2 \sin^2\theta)$ which is related to the effect density gradient and axial symmetry have in the evolution of the magnetic field. The vector equation giving the evolution of the magnetic field reduces to

$$\frac{\partial \Psi}{\partial t} = r^2 \sin^2\theta\ \chi(\nabla\Psi \times \nabla I)\cdot\nabla\phi + \frac{c^2}{4\pi\sigma}\Delta^*\Psi\,, \tag{2.2}$$

$$\begin{aligned}\frac{\partial I}{\partial t} &= r^2\sin^2\theta[\chi\nabla(\Delta^*\Psi)\times\nabla\Psi + \Delta^*\Psi\nabla\chi\times\nabla\Psi + I\nabla\chi\times\nabla I]\cdot\nabla\phi \\ &\quad + \frac{c^2}{4\pi\sigma}\left(\Delta^* I + \frac{1}{\sigma}\nabla I \times \nabla\sigma\right).\end{aligned} \tag{2.3}$$

These two equations form a system of non-linear, coupled, differential equations for Ψ and I, which in principle can be solved numerically. Yet, by analytical examination of the above equations we can come to some important conclusions. Assuming high conductivity σ, it is possible to find Hall equilibria solutions satisfying $\frac{\partial\Psi}{\partial t} = \frac{\partial I}{\partial t} = 0$, these solutions have $I = I(\Psi)$ with Ψ satisfying a Grad-Shafranov equation, similar to that of barotropic magnetic equilibria (Cumming *et al.* 2004; Gourgouliatos *et al.* 2013a,b). In the absence of an initial poloidal field ($\Psi = 0$), the toroidal field evolves with the advection of I on surfaces of constant χ obeying Burgers' equation (Reisenegger *et al.* 2007). However, a purely poloidal initial field generates a toroidal field, even if it is not present in the initial state.

3. Simulation - Conclusions

We have developed a finite difference code to study the evolution of the magnetic field because of the Hall effect and Ohmic dissipation. We assume that the electron number density on the surface of the crust is two orders of magnitude smaller than in the crust-core interface and it is $n_{\rm e} \propto (r_* - r)^4$, while the conductivity is $\sigma \propto n_{\rm e}^{2/3}$, the thickness of the crust is $0.2r_*$, where r_* is the radius of the neutron star. The field is confined in the crust of the neutron star without threading the core, while the star is surrounded by a vacuum, therefore, a multipole expansion is used as a surface boundary condition. We have also run cases with constant electron number density $n_{\rm e}$ to allow comparison with previous studies. We have run a variety of initial conditions: purely toroidal field (Figure 1), purely poloidal fields and combinations of poloidal and toroidal fields.

We link the analytical conclusions with the results of our simulations. In particular, a purely toroidal field is advected along lines of constant χ. A Hall equilibrium field does not evolve in a Hall timescale, but in a longer timescale which depends on the Ohmic

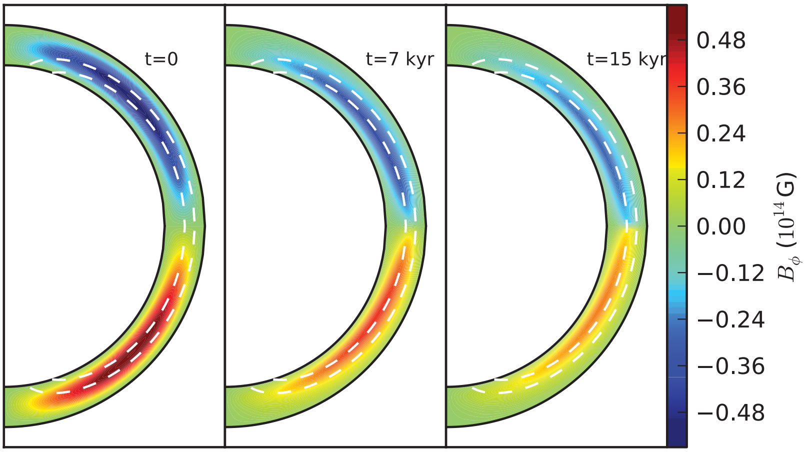

Figure 1. The evolution of a purely toroidal field. I is advected along surfaces of constant χ, drawn with white dashed lines. Within a Hall time-scale shocks form between fields of opposite polarity. For a colour figure please refer to the online version.

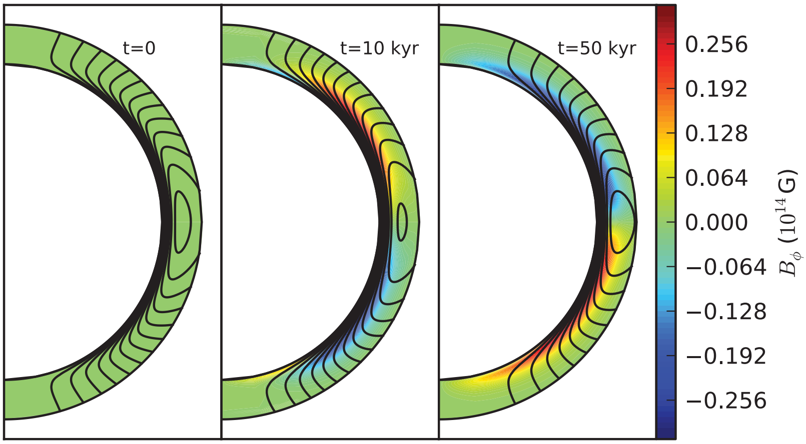

Figure 2. The evolution of poloidal field starting out of Hall equilibrium so that it generates a toroidal field of positive polarity in the northern hemisphere. The field lines are pushed towards the poles initially. For a colour figure please refer to the online version.

timescale. Ohmic dissipation pushes the field out of Hall equilibrium, thus a toroidal field is generated. A purely poloidal field out of Hall equilibrium generates a toroidal field within a Hall timescale. The polarity of the toroidal field generated and subsequent evolution depends on the initial field structure compared to the Hall equilibrium field. If the quadrupolar toroidal field is positive in the northern hemisphere the poloidal field lines are pushed to the poles (Figure 2), otherwise the poloidal field lines are pushed to the equator (Figure 3), leading to distinguishable structures. The toroidal field is subdominant energetically compared to the poloidal, unless the initial conditions impose a strong toroidal field (Ciolfi & Rezzolla 2013). A strong toroidal field twists the poloidal field lines trying to align I with Ψ, while transferring a significant amount of energy to the poloidal field. Assuming a density profile where χ =const. the field generates higher order multipoles, which are suppressed otherwise.

The two evolutionary paths shown in Figures 2 and 3 can be distinguished observationally in terms of the braking indices as they predict different decay rates for the

https://doi.org/10.1017/S1743921314002634 Published online by Cambridge University Press

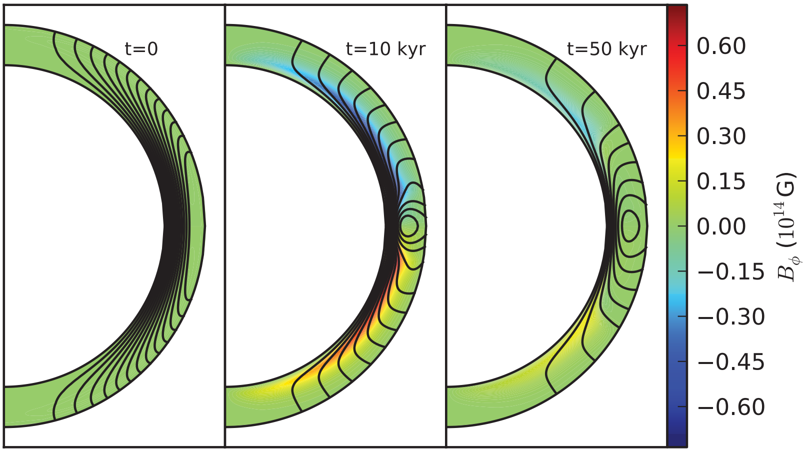

Figure 3. The evolution of poloidal field starting out of Hall equilibrium so that it generates a toroidal field of negative polarity in the northern hemisphere. The field lines are pushed towards the equator. For a colour figure please refer to the online version.

dipole component of the field. Also the surface temperature profile is different, as thermal conductivity depends on the internal structure of the field (Viganò *et al.* 2013).

Acknowledgements

KNG is supported by the Centre de Recherche en Astrophysique du Québec. AC is supported by an NSERC Discovery Grant and is an Associate Member of the CIFAR Cosmology and Gravity Program.

References

Biskamp, D., Schwarz, E., & Drake, J. F. 1996, *Physical Review Letters*, 76, 1264
Cho, J. & Lazarian, A. 2009, *ApJ*, 701, 236
Ciolfi, R. & Rezzolla, L. 2013, *MNRAS*, 435, L43
Cumming, A., Arras, P., & Zweibel, E. 2004, *ApJ*, 609, 999
Goldreich, P. & Reisenegger, A. 1992, *ApJ*, 395, 250
Gourgouliatos, K. N., Cumming, A., Reisenegger, A., *et al.* 2013, *MNRAS*, 434, 2480
Gourgouliatos, K. N., Cumming, A., Lyutikov, M., & Reisenegger, A. 2013, arXiv:1305.0149
Hollerbach, R. & Rüdiger, G. 2002, *MNRAS*, 337, 216
Hollerbach, R. & Rüdiger, G. 2004, *MNRAS*, 347, 1273
Jones, P. B. 1988, *MNRAS*, 233, 875
Kojima, Y. & Kisaka, S. 2012, *MNRAS*, 421, 2722
Olausen, S. A. & Kaspi, V. M. 2013, arXiv:1309.4167
Pons, J. A. & Geppert, U. 2007, *A&A*, 470, 303
Reisenegger, A., Benguria, R., Prieto, J. P., Araya, P. A., & Lai, D. 2007, *A&A*, 472, 233
Shalybkov, D. A. & Urpin, V. A. 1997, *A&A*, 321, 685
Vainshtein, S. I., Chitre, S. M., & Olinto, A. V. 2000, *Phys. Rev. E*, 61, 4422
Viganò, D., Pons, J. A., & Miralles, J. A. 2012, Computer Physics Communications, 183, 2042
Viganò, D., Rea, N., Pons, J. A., *et al.* 2013, *MNRAS*, 434, 123
Wareing, C. J. & Hollerbach, R. 2009, *A&A*, 508, L39